

Multi-wall carbon nanotubes as quantum dots

M. R. Buitelaar, A. Bachtold,* T. Nussbaumer, M. Iqbal, and C. Schönenberger†

*Institut für Physik, Universität Basel,
Klingelbergstr. 82, CH-4056 Basel, Switzerland*

Abstract

We have measured the differential conductance dI/dV of individual multi-wall carbon nanotubes (MWNT) of different lengths. A cross-over from wire-like (long tubes) to dot-like (short tubes) behavior is observed. dI/dV is dominated by random conductance fluctuations (UCF) in long MWNT devices ($L = 2 \dots 7 \mu\text{m}$), while Coulomb blockade and energy level quantization are observed in short ones ($L = 300 \text{ nm}$). The electron levels of short MWNT dots are nearly four-fold degenerate (including spin) and their evolution in magnetic field (Zeeman splitting) agrees with a g -factor of 2. In zero magnetic field the sequential filling of states evolves with spin S according to $S = 0 \rightarrow 1/2 \rightarrow 0 \dots$. In addition, a Kondo enhancement of the conductance is observed when the number of electrons on the tube is odd.

PACS numbers: 73.61.Wp, 73.63.Fg, 73.63.Nm, 73.63.Kv, 73.21.La, 73.23.Hk, 72.15.Qm

*Present address TUDelft, 2628 CJ Delft, Netherlands.

†Electronic address: Christian.Schoenenberger@unibas.ch; URL: www.unibas.ch/phys-meso

Carbon nanotubes (NTs) are excellent model systems to study the electronic properties of low-dimensional conductors [1]. Transport and scanning probe measurements on metallic single-wall nanotubes (SWNT, diameter $d \sim 1$ nm) have revealed that these are one-dimensional conductors (1D) with long mean free paths, $l_{mfp} > 1 \mu\text{m}$ [2, 3, 4]. In contrast, multi-wall carbon nanotubes (MWNT, outer diameter $d \sim 15$ nm) [5], which are composed of a set of coaxial NTs, were found to be disordered. The transport regime varied from 2D-diffusive in some MWNTs ($l_{mfp} \lesssim 10$ nm) [6, 7], to quasi-ballistic in others ($l_{mfp} \sim 100$ nm) [8]. Most SWNT devices, even very long ones with lengths $L \sim 1 \mu\text{m}$, have displayed single-electron tunneling effects [9] with conventional Coulomb blockade oscillations and a quantization of the electron states (particle-in-a-box) at $T \lesssim 10$ K [2, 3]. This demonstrates that the SWNTs were only weakly coupled to the leads in these experiments. The very fact that transport occurs through discrete electron states implies that the corresponding molecular orbitals are phase-coherent and extend over long distances, a remarkable result for a 1D electron system. Very recently, highly transparent contacts to SWNTs could be realized [10]. The physics of these systems proved to be very rich and ranges from devices dominated by higher-order co-tunneling processes (like e.g. the Kondo effect) at intermediate contact transparencies $T \sim 0.1 - 0.5$ [11] to open ballistic systems with transparencies approaching unity [10].

While there are many examples of SWNT quantum dots, little effort has been gone into the investigation of MWNTs as such systems. Given the larger size, the corresponding smaller energy scales and, most notably, the intrinsic scattering, it is not obvious that these experiments will lead to the same results. As we will show below it turns out that in many respects they do. Since the level spacing δE scales inversely with length, quantum dot features will be most pronounced in short devices. We have therefore studied MWNTs with short 300 nm inter-electrode spacing. We report here measurements of one such device which showed pronounced quantum dot features. For comparison we have also investigated the linear-response conductance of a very long MWNT (7.4 μm).

Figure 1 shows the dependence of the conduction G of a 300 nm long MWNT device as a function of gate voltage (backgate). Details on device fabrication can be found in Ref. [8]. Large and reproducible fluctuations of order e^2/h develop in G . Note, that the average conductance is quite large, i.e. $\langle G \rangle > 2e^2/h$, and nearly temperature independent. The root-mean square δG_{rms} of the conductance fluctuations $\delta G = G - \langle G \rangle$ is displayed in the

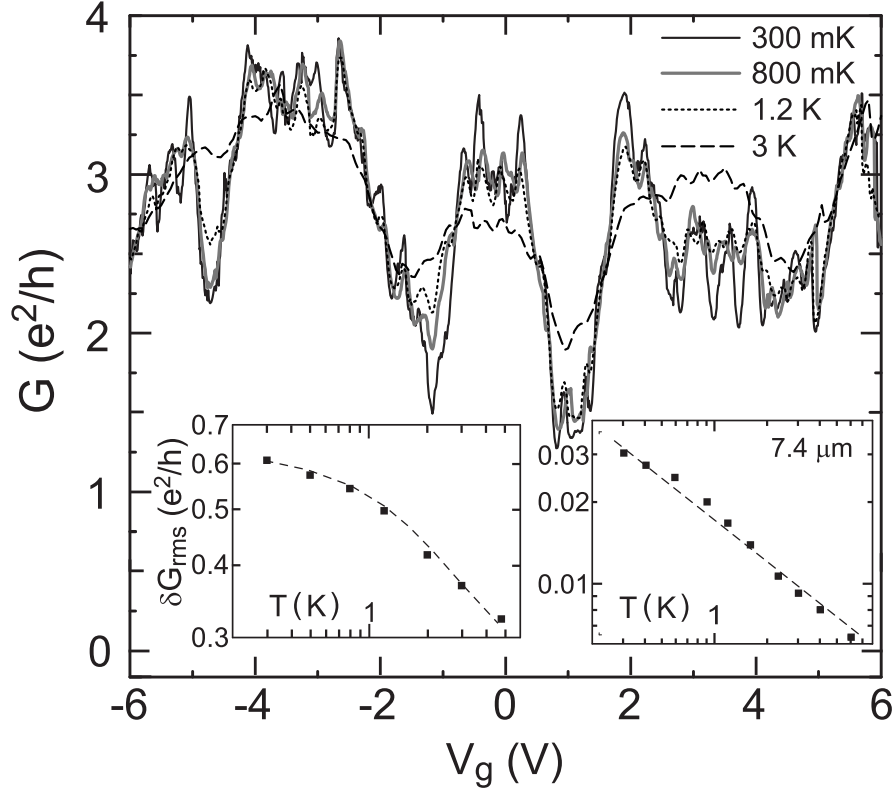


FIG. 1: Linear response conductance G as a function of gate voltage V_g (backgate) at temperatures between 280 mK and 3 K for a MWNT with contacts separated by 300 nm. Lower left inset: the corresponding root-mean square δG_{rms} of the conductance fluctuations $\delta G = G - \langle G \rangle$. Lower right inset: as a reference, δG_{rms} of a very long MWNT device with inter-electrode spacing of 7.4 μm . The temperature dependence obeys $\delta G_{rms} \propto T^{-1/2}$ (dashed line).

lower left inset as a function of temperature T . For disordered wires random variations of G as a function of magnetic field or Fermi energy (which is changed here by the gate) are usually assigned to universal conductance fluctuations (UCF). These fluctuations depend on the specific scattering potential but are universal in the sense that their amplitude at zero temperature is of order e^2/h , regardless of the sample size and degree of disorder. At finite temperature, self-averaging reduces δG_{rms} . For a wire which is 1D with respect to the phase-coherence length l_ϕ it is given by: $\delta G_{rms} = \sqrt{12}(e^2/h)(l_\phi/L)^{3/2}$, where $L \gg l_\phi$ is the wire length [12]. When l_ϕ becomes of the order of L , there is a cross-over to the universal value, $\delta G_{rms} = 0.73e^2/h$ [12]. The cross-over appears in the measurement at $T \lesssim 1\text{ K}$ and $\delta G_{rms} \approx 0.6e^2/h$ at $T_0 = 280\text{ mK}$, in good agreement with theory. At this temperature the

average conductance amounts to $2.8e^2/h$. The saturation of δG_{rms} close to the universal limit suggests conduction through one phase coherent unit. This in turns implies that $l_\phi \gtrsim L$.

As a comparison, we also show $\delta G_{rms}(T)$ of a long MWNT with $L = 7.4 \mu\text{m}$ in the lower right inset of Fig. 1 For this long nanotube device, $l_\phi/L \ll 1$, which is reflected in the much smaller amplitude of δG_{rms} . $\delta G_{rms} = 0.03e^2/h$ at T_0 corresponds to $l_\phi = 320 \text{ nm}$. This is consistent with the estimate of l_ϕ for the short MWNT and also agrees with l_ϕ deduced from magneto-conductance experiments of other MWNT samples [8]. The dephasing mechanism can be determined from the measured temperature dependence of l_ϕ . Since δG_{rms} follows a power-law in T over more than one decade with an exponent close to $-1/2$ (line in the lower right inset of Fig. 1), $l_\phi(T) \propto T^{-1/3}$. This is the behavior expected for a quasi-1D conductor. The main contribution to phase-breaking is caused by electron-electron collisions with small energy transfers, a process known as Nyquist dephasing [13].

In terms of l_ϕ the long NT is a wire, whereas the short one is a dot for which Coulomb blockade (CB) may be important. We now estimate the single-electron charging energy $U_C = e^2/C$ [14] for the latter and compare it with the base measuring temperature $T_0 = 0.28 \text{ K}$. The dominant contribution to the electrostatic capacitance C of short MWNTs is due to the contacts, leading to $C \sim 400 \text{ aF}$ (see below). Hence, $U_C \sim 4.6 \text{ K}$, i.e. $U_C/kT_0 \sim 17$, and CB is therefore expected. This, however, does not seem to be the case: firstly, the average conductance $\langle G \rangle$ is nearly temperature independent (also over a larger temperature range than shown in the graph); secondly, the conductance is large $\langle G \rangle = 2.8e^2/h$; and thirdly, G lacks the periodicity in gate voltage expected for a weakly coupled quantum dot. We attribute the absence of clear CB features to a large contact transparency. With increasing gate voltage from 0 to 14 V, however, the average conductance decreases from $2.8e^2/h$ to $\sim 2e^2/h$, possibly reflecting a decreasing contact transparency. This assumption is supported by the following measurement which displays clear Coulomb blockade features in the large gate-voltage regime. Fig. 2 shows a grey-scale representation of dI/dV versus gate voltage V_g (horizontal) and transport voltage V_{sd} (vertical) in the regime $V_g = 14 \dots 17 \text{ V}$. Although the overall two terminal conductance is still large, i.e. $G \sim 2e^2/h$, the ‘remainders’ of CB are clearly visible. The most striking observation is a sequence of a large low-conduction CB ‘diamond’ followed by 3 smaller ones (best seen on the left). The diamonds are highlighted by dashed lines in the figure. The size of the CB-diamonds reflects the magnitude of the addition energy ΔE_{add} , which measures the difference in chemical potential of two adjacent

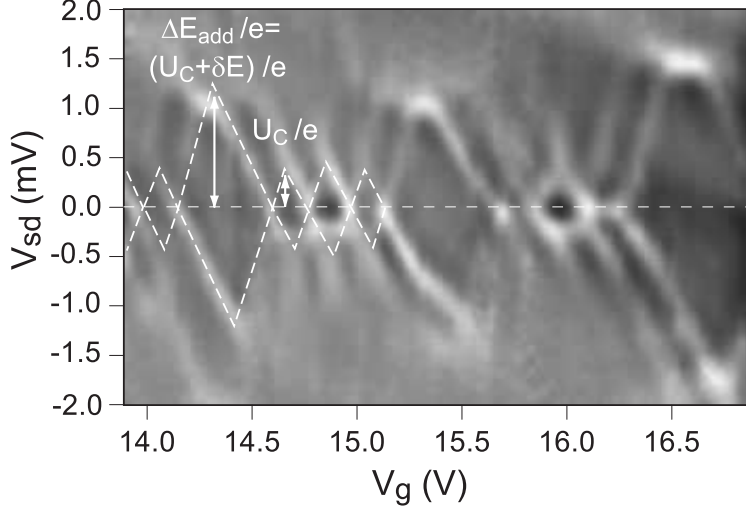


FIG. 2: Greyscale representation of the differential conductance as a function of source-drain (V_{sd}) and gate voltage (V_g) at 280 mK (lighter = more conductive). The average 2-terminal conductance is high ($\sim 2e^2/h$), nevertheless clear traces of Coulomb blockade are observed. The pattern of a large ‘diamond’ followed by 3 smaller ones suggest a (nearly) 4-fold degeneracy (including spin) of the single-electron dot states. ΔE_{add} , U_C , and δE denote the addition energy, the charging energy $U_C = e^2/C$, and the single-electron level spacing, respectively.

charge states of the dot [9]. In the constant interaction model (C independent of N) $\Delta E_{add} = U_C + \delta E$. If all the single-electron levels would repel each other (only 2-fold spin degeneracy) and $\delta E \sim U_C$, an alternating sequence of small and large CB diamonds would be expected. Starting from an even filling number, $\Delta E_{add} = U_C + \delta E$ for the first added electron (large diamond) and to U_C for the second one (small diamond) [11]. The sequence of one large diamond, followed by three smaller ones of approximate equal size, which is observed here, suggests that the degeneracy of the states is not 2, but rather 4 (including spin). From the size of the diamonds we obtain $\delta E = 0.8$ meV and $U_C = 0.4$ meV, the latter corresponding to $C = 400$ aF. The total capacitance C is the sum of the gate capacitance C_g and the contact capacitances C_l (left) and C_r (right). All three parameters can be deduced from the diamonds. We obtain: $C_g = 1$ aF and $C_{l,r} = 260, 140$ aF.

The level spacing δE of an ideal metallic SWNT is given by $\delta E = \hbar v_F/2L$, where v_F is the Fermi velocity [5, 15]. This holds for an undoped NT. Recently, it has been found that MWNTs are substantially hole-doped by the environment [16]. As a consequence more

than the ideally expected 2 modes participate in transport. Hence, $\delta E = hv_F/ML$, where $M > 2$ is the number of 1D subbands. Taking $v_F = 8 \cdot 10^5$ m/s [17], the measured value of $\delta E = 0.8$ meV corresponds to $M \approx 14$, in good agreement with Krüger *et al.* [16]. An estimate of the lifetime broadening Γ can be obtained from the measured width of the Coulomb peaks and yields $\Gamma \approx 0.25$ meV.

The observed 4-fold degeneracy can be explained by a specific property of the graphite sheet (graphene). In the simplest tight-binding band-structure calculation all 1D-bands are twofold degenerate (not including spin) [15]. This degeneracy can be traced back to the presence of two C-atoms per unit cell, each contributing with one valence orbital. This, so-called K-K'-degeneracy has not been observed before, although it is supposed to be a *generic* feature of graphene.

To explore this scenario further we have also studied the gate-voltage shifts of the linear-response conductance peaks as a function of a perpendicular magnetic field B , Fig. 3. The difference between the positions of adjacent peaks can also be related to the addition energy: $\Delta V_g = C\Delta E_{add}/eC_g$. Figure 3a shows the evolution in small magnetic field $B \leq 3$ T. Adjacent peaks are seen to shift in opposite directions. This is the behavior of a ground-state whose spin alternates as $S = 0 \rightarrow 1/2 \rightarrow 0 \dots$. This, however, contradicts the assumed 4-fold degeneracy for the following reason: In the presence of a magnetic field the energy of an electron depends on its spin due to the Zeeman effect which lowers the degeneracy from 4 to 2 (only Zeeman energy assumed). For $N = 2$, the two electrons are thus expected to occupy different orbitals with *parallel* spins. Actually, this would already be expected for $B = 0$, because of exchange-correlation (Hund's rule would favour the spin-triplet with total angular momentum $S = 1$) [18]. The spin should therefore evolve as $S = 1/2 \rightarrow 1$ for $N = 1 \rightarrow 2$. Experimentally, however, the first 2 electrons have opposite spins and are thus added to the same orbital state. This discrepancy can only be resolved, if the assumed 4-fold degeneracy is not 'exact', i.e. there are pairs of states which lie close together with spacing δE^* . The pairs themselves are spaced by $\delta E > \delta E^*$. A detailed study of the peak evolutions (Fig. 3b) reveals that this is indeed the case. ΔE_{add} at $B = 0$ of the $2 \rightarrow 3$ ($6 \rightarrow 7$) transition is clearly larger than the $1 \rightarrow 2$ and $3 \rightarrow 4$ ($5 \rightarrow 6$ and $7 \rightarrow 8$) ones. We obtain $\delta E_{23}^* \approx 0.1$ meV and $\delta E_{67}^* \approx 0.18$ meV, on average $\delta E^* \approx 0.14$ meV. We have also verified that the energy shifts agree with the Zeeman term for electrons occupying the same orbital. We plot in Fig. 3c the corresponding addition energies as a function of B . A best

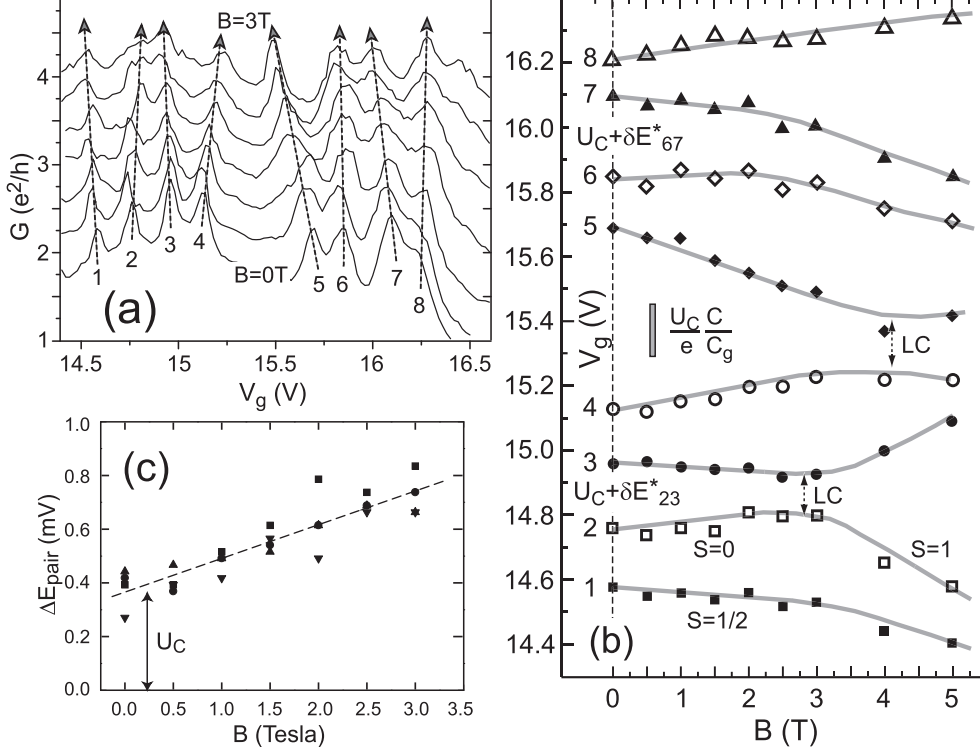


FIG. 3: (a) Linear-response conductance G as a function of gate voltage V_g for different magnetic fields $B = 0 \dots 3$ T (vertically offset for clarity). The evolution of the conductance peaks are highlighted by dashed lines. (b) Peak positions versus $B = 0 \dots 5$ T. Curves are guides to the eye and LC denotes level-crossings. (c) Magnetic field dependence of the addition energy δE_{pair} deduced from the separation of adjacent peaks involving electrons on the same orbital (the pairs $1 \leftrightarrow 2$, $3 \leftrightarrow 4$, $5 \leftrightarrow 6$, and $7 \leftrightarrow 8$). The dashed line (least-square fit) corresponds to the Zeeman energy with Landé factor $g = 2.1$.

fit of the data to $U_C + g\mu_B B/e$, where μ_B is the Bohr magneton and g the Landé factor, is shown as a dashed line and yields $g = 2.1 \pm 0.3$. This value is consistent with $g = 2.0$ for graphite and with previous measurements of g for a SWNT [2, 21].

In high magnetic field levels cross. Two crossings (LCs) are seen in Fig. 3b. At ≈ 3 T, for example, the spin-up of the first orbital crosses the spin-down of the second, giving rise to an $S = 0 \rightarrow 1$ transition. A similar crossing is not seen in the upper part. On the one hand, this is due to the larger δE^* . On the other hand, there is also a magnetic-field dependence of the orbitals which increases δE^* at higher fields.

We find a pattern that repeats every 4th electron due to an apparent *pairing* of orbital

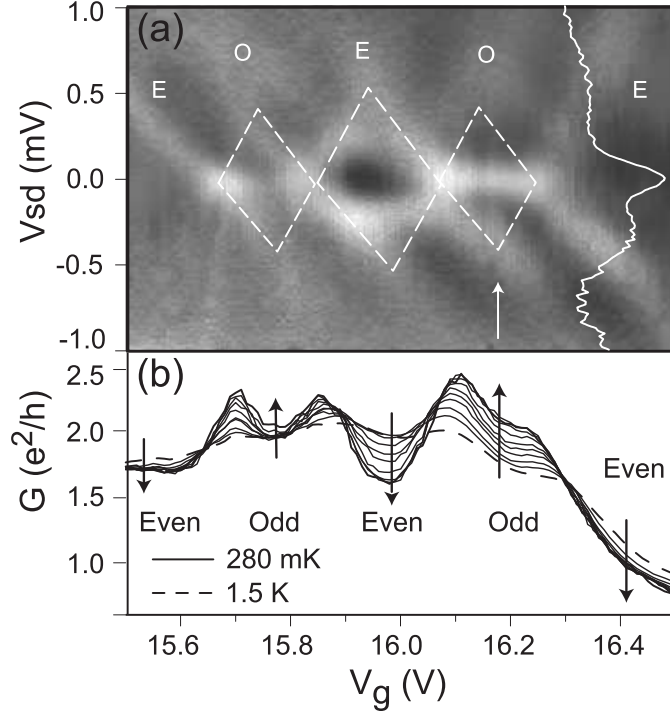


FIG. 4: (a) Greyscale representation of dI/dV as a function of source-drain (V_{sd}) and gate voltage (V_g) at 280 mK (lighter = more conductive). Within regions marked as O (E) the number of electrons on the tube is odd (even). The horizontal features (best seen in outer right diamond) are caused by the Kondo effect. (b) Temperature dependence of the linear-response conductance. The arrows indicate directions of decreasing temperature.

states. We believe that this pairing is related to the $K - K'$ -degeneracy. The splitting δE^* is proposed to be caused by hybridization via the contacts, which are strongly coupled to the NT. We expect a level ‘repulsion’, in size comparable to the life-time broadening, which we estimated to be $\Gamma \approx 0.25$ meV. This is in fair agreement with $\delta E^* \approx 0.14$ meV. In high magnetic field the intrinsic $K - K'$ -degeneracy should be lifted which enhances the level separation further. This may explain why the $S = 0 \rightarrow 1$ transition is not observed for the upper quartet in Fig. 3b. Finally, the fact that $S = 0$ for $N = 2$ at $B = 0$ is only consistent with Hund’s rule if the exchange energy $E_X < \delta E^*$, yielding an upper bound for E_X of 0.14 meV.

Another interesting manifestation of the electron spin on the electronic transport can be seen in the gate region between 15.5 and 16.5 V. We have measured this part with improved accuracy and it is shown in Fig. 4. Fig. 4b shows the linear-response conductance. In

the valleys marked as E (even filling) the conduction decreases with decreasing temperature while it increases in the valleys marked as O (odd filling). Contrary to what one might expect from normal CB, a high conduction ‘ridge’ around $V_{sd} = 0$ V develops in the latter (best seen in the right most diamond). These observations can be understood with the Kondo model [11, 19, 20]. When the number of electrons on the tube is odd and the coupling to the leads is sufficiently strong a spin singlet can form between the spin polarized tube and electrons in the leads. This results in a resonance in the density-of-states at the Fermi energy (i.e. the Kondo resonance). The width of the Kondo resonance reflects the binding energy of the singlet which is usually described by a Kondo temperature T_K . The conductance is expected to increase logarithmically with decreasing temperature in the centers of the ridges below T_K . Following G as a function of temperature at $V_g = 16.2$ V we indeed find a logarithmic dependence between 280 mK and 1 K. At temperatures well below T_K the conductance is expected to saturate at a maximum value of $2e^2/h$. This is called the unitary limit. In our case, however, no saturation has been observed down to 280 mK.

The Kondo effect is expected to be suppressed by a small bias voltage across the tube of the order of $\pm k_B T_K / e$. The ridge at $V_g = 16.2$ V has a width of ~ 0.2 meV which would correspond to $T_K = 1.2$ K (see curve in Fig. 4a). This is roughly in agreement with the onset of the logarithmic increase of G below ~ 1 K. An additional prediction is the disappearance of the Kondo resonance in a magnetic field. The high conductance ridge indeed broadens and disappears above ~ 1.5 T. Simultaneously, the Coulomb blockade diamonds are recovered.

We acknowledge W. Belzig, G. Burkard, D. Cobden, R. Egger and J. Nygård for discussions. We thank L. Forró for the MWNT material and J. Gobrecht for providing the oxidized Si substrates. This work has been supported by the Swiss NFS.

-
- [1] For reviews, see: C. Dekker, *Physics Today* **52** (5), p22-28 (1999); C. Schönberger and L. Forró, *Physics World*, June 2001, p37-41.
 - [2] S. J. Tans *et al*, *Nature* **386**,474 (1997).
 - [3] M. Bockrath *et al*. *Science* **275**, 1992 (1997).
 - [4] A. Bachtold *et al.*, *Phys. Rev. Lett.* **84**, 6082 (2000).
 - [5] L. Forró and C. Schönberger in *Carbon Nanotubes*, edited by M.S. Dresselhaus, G. Dressel-

- haus and Ph. Avouris, Topics in Applied Physics, Vol.80 (Springer 2001).
- [6] L. Langer *et al.*, Phys. Rev. Lett. **76**, 479 (1996).
 - [7] A. Bachtold *et al.*, Nature **397**, 673 (1999).
 - [8] C. Schönenberger, A. Bachtold, C. Strunk, J.-P. Salvetat and Forró, Appl. Phys. A **69**, 283 (1999).
 - [9] L.P. Kouwenhoven *et al.*, in *Mesoscopic Electron Transport*, edited by L.P. Kouwenhoven, G. Schön, and L.L. Sohn (Kluwer, Dordrecht, The Netherlands, 1997).
 - [10] W. Liang *et al.*, Nature **411**, 665 (2001).
 - [11] J. Nygård, D.H. Cobden, and P. E. Lindelof, Nature **408**, 342 (2000).
 - [12] P.A. Lee, A.D. Stone, and H. Fukuyama, Phys. Rev. B **35**, 1039 (1987); P.A. Lee and A.D. Stone, Phys. Rev. Lett. **55**, 1622 (1985).
 - [13] B. L. Altshuler, A. G. Aronov, and D. E. Khmel'nitsky, J. Phys. C **15**, 7367 (1982).
 - [14] For convenience we use $U_C = e^2/C$ instead of $E_C = e^2/2C$.
 - [15] See e.g., M. S. Dresselhaus, G. Dresselhaus, P. C. Eklund: *Science of Fullerenes and Carbon Nanotubes* (Academic Press, New York 1996).
 - [16] M. Krüger, M. Buitelaar, T. Nussbaumer, and C. Schönenberger, Appl. Phys. Lett. **78**,1291 (2001).
 - [17] The Fermi velocity of $8 \cdot 10^5$ m/s is an upper limit since the average v_F might be lower for a system doped into several subbands.
 - [18] S. Tarucha, D.G. Austing, Y. Tokura, W.G. van der Wiel, and L.P. Kouwenhoven, Phys. Rev. Lett. **84**, 2485 (2000).
 - [19] For a review see: L. Kouwenhoven and L. Glazman in Physics World, January 2001, p.33-38.
 - [20] D. Goldhaber-Gorden *et al.*, Nature **391**, 156 (1998).
 - [21] D. H. Cobden, M. Bockrath, P.L. McEuen, A.G. Rinzler, and R.E. Smalley, Phys. Rev. Lett. **81**, 681 (1998).